Mechanical strength and defect distributions in flash sintered 3YSZ

João Gustavo Pereira da Silva [a], Amir Nazari Yamchelou [a], Audrey Debris [b],
Christian Wieck [a], Hans Jelitto [a], Hazim Ali Al-Qureshi [c], Rolf Janssen [a,*]

[a] Technische Universitat Hamburg-Harburg, Hamburg, Germany
[b] Institut Catholique d'Arts et Metiers, France
[c] Universidade Federal de Santa Catarina, Joinville, Brazil

ARTICLE INFO

ABSTRACT

The influence of preexisting defects and the generation of new ones during flash sintering was studied in 3YSZ. Weibull statistics was used to analyse mechanical testing data from flash and conventionally sintered specimens with equal densification. The obtained values for Weibull modulus and characteristic strength are 6.09 and 371 MPa for the conventionally sintered samples, respectively, and 5.92 and 506 MPa for the flash sintered samples. It can be inferred that flash sintering does not alter significantly the defect distribution on the studied material. Preexisting defects were manufactured with rice starch as a pore forming agent, in 5, 10 and 15 vol%. Those samples were flash sintered in isothermal and constant heating rate experiments. The experiments show that there is no noticeable difference on the incubation time and the onset temperature for flash sintering.

1. Introduction

Flash sintering is a recently developed method in which ceramics can be sintered at low temperatures in a short time. It is a non-linear phenomenon, characterized by an incubation period (Stage 1) followed by a sharp increase of the conductivity of the sample and simultaneous rapid heating under an electric field above a threshold temperature (Stage II), usually followed by a constant current hold time (Stage III) [1].

The method was first reported in 2010, with Yttria-stabilized Zirconia (YSZ) [2], which is an ionic conductor, but has been observed in a wide range of conductivities, as from a poor conductor such as MgO doped Alumina [3] to highly conductive Cobalt Manganese Spinel [4]. It seems that the material conductivity is directly correlated to the threshold of critical electrical field temperature which leads to flash sintering. However, detailed data on conductivity of ceramics and the conduction mechanisms in the temperature range (400–1200 °C) and the electrical field range (50–2000 V/cm) leading to flash sintering it is still an open point to be investigated.

The main mechanisms of flash sintering are still not well understood. Most of the attempts to explain the phenomenon are related to a sintering process activated via Joule heating [5] or local melting at the grain boundaries [6], but recent results and discussions have

led to conclusions indicating that the temperatures obtained during flash sintering could not be high enough to explain thereby the densification behaviour [7,8]. New mechanisms, such as the nucleation of defect embryos under the effect of polarization by the field, have been proposed to account for both the higher conductivity and self-diffusion (sintering) observed [9].

Since the first experiments on flash sintering an inhomogeneous light emission in the ceramic was observed. It is still debatable whether this emission is related to Joule heating or other phenomena, such as defect recombination [10]. In theory, that effect can be related to local defects on the green body. And since one of the earlier reports has shown the effects of particle size [11], that brought up the question, of how far the preexisting defects on a ceramic material have influence on their behaviour in the flash sintering process.

Another related subject is that the mechanical properties of flash sintered specimens were not given due attention in recent studies. The only report up to date on the mechanical properties of flash sintered samples [12] was conducted with a small amount of samples (10), so the Weibull parameters, and therefore the defect distribution cannot be estimated.

The present paper concerns itself on the influence of defects pre and post flash sintering. Therefore specimens with defined defects were produced and flash sintered. Also, extensive mechanical testing was conducted with conventionally and flash sintered 3YSZ. From the Weibull parameters, the defect distribution post flash is estimated and compared with SEM pictures.
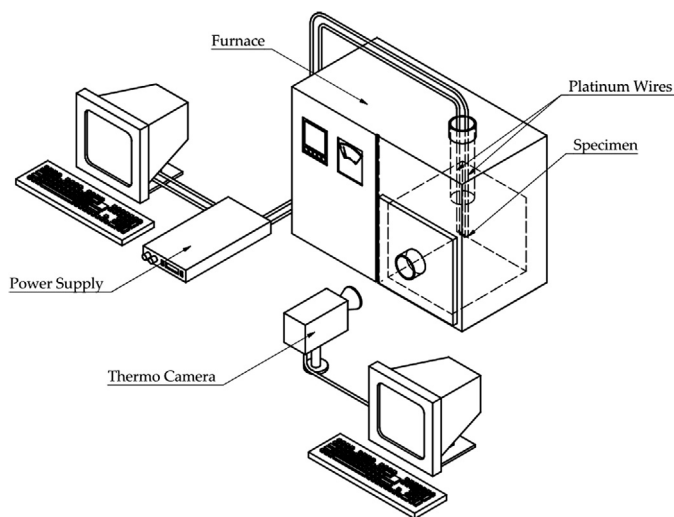

Fig. 1. Set up of the furnace for the flash sintering experiments.

2. Experimental

Samples were fabricated with a mixture of 3% Yttria Stabilized Zirconia powder (Tosoh 3Y-E, Japan) with 2 wt% binder (PVA) and distilled water, and mixed on a ball mill for at least 4 h. The mixture was then dried in an oven at 90 °C, and ground again to a powder in a mortar and pestle. Part of the powder was mixed with 5, 10 and 15 vol% of rice starch as pore former, having a maximum agglomerate size of 125 μm in diameter. The powders were uniaxially pressed (100 MPa) in the shape of dogbones with a cross section of 4 mm × 2 mm and cold isostatically pressed (200 MPa) to a relative green density of 50–52%. The binder and pore former removal was carried out in an oven for at least 3 h at 700 °C.

For the flash sintering experiments a modified chamber furnace *Nabertherm HT 04/17* was used (Fig. 1). The electrical connections, supplied by platinum wires with a diameter of 1 mm, went through the ceiling of the chamber in a ceramic tube with an inner diameter of 37 mm. The specimen was placed in the middle of the furnace chamber and then hooked to the platinum wires. The contact area between the specimen and the platinum wires was covered with silver paste, to ensure a good electrical contact and facilitate a uniform current density through the section of the specimen. Voltage and current were controlled by a *Sorensen DLM 300-2* power supply connected to the platinum wires. To control and record the voltage and current curves the power supply was connected to a computer. The software used for data acquisition was *Labview*. The voltage and current measurements were recorded with an acquisition rate of four measuring points per second.

Another tube with an inner diameter of 37 mm went through the front of the chamber, to allow a thermal camera to record the flash sintering. The camera used was a *HDRC Q-PyroCam*. These recordings were needed for the experiments with constant voltage with rising oven temperature. The temperature at the flash event was given by the internal measurement unit of the furnace.

The flash sintering experiments for the samples with pore forming agents were separated into two runs. In the first part, isothermal experiments were conducted. In these experiments the oven temperature was held constant at 750 °C, 850 °C or 950 °C. An electrical field of 62.5 V/cm, 75 V/cm, 87.5 V, 100 V/cm or 112.5 V/cm was applied onto the specimens instantly. Voltage and current were recorded and the time from the application of the voltage to the onset of the flash sintering, i.e. the incubation time, was measured.

In the second part the experiments with constant electrical field of 62.5 V/cm, 75 V/cm, 87.5 V/cm, 100 V/cm or 112.5 V/cm and a

constant heating rate of 10 °C/min were performed. The oven was pre set to a starting temperature of 600 °C when the voltage was applied. Then the temperature was increased until the threshold conditions for flash sintering were reached. The oven temperature at that moment was recorded.

For the mechanical testing, 36 specimens of each processing condition were manufactured. 36 specimens were fabricated by isothermal flash sintering, using the following parameters: furnace temperature of 900 °C, electrical field of 100 V/cm, hold time of 60 s and maximum current density of 10 A/cm^2. 36 specimens with the same final density (94% TD) were manufactured via conventional sintering, on a heating schedule of 10 °C/min, and a holding step at 1280 °C for 90 min, followed by cooling down on the furnace by turning off the heating elements. Those conditions were used due to being the most reproduceable with our experimental setup.

Flexural testing of the samples was carried out on a bending machine [13]. Since the length of the specimens was not suitable for a 4-point bending test, necessary adjustments were made to adapt the machine to the limited length of the samples. 32 samples of each sintering condition were tested in simple 3-point bending with a support distance of 7 mm for the determination of the Weibull parameters and 4 samples each were notched with a razor blade and subjected to 3-point bending in order to measure the fracture toughness.

The bending machine consists of mainly a rigid rectangular frame and two separate bolts. These bolts provide the necessary load required to cause a fracture in a specimen. The secondary bolt has a sole function of creating contact with a specimen, while the primary bolt, which is loosened and tightened through a wheel manually as well as through a stepper motor (not shown in the figure) automatically. The primary bolt brings the load on the sample by pressing on the secondary bolt. Through a flexible plastic plate, the second bolt, before loading, is held floating between the primary bolt and a load sensor. The plastic plate provides a certain level of flexibility, so that the force created by the second bolt on the specimen during contact creating is limited to 2 [N] or 3 [N]. Through horizontal adjustment of the parallelogram frame, the point of loading is exactly placed in the middle of the two supporting points, which lie underneath the specimen. The parallelogram is lifted through a counterweight (not shown in the figure), so that the weight of the parallelogram is fully compensated. Measurement of the applied load is facilitated through a load sensor, and bending of the specimen through an inductive position sensor.
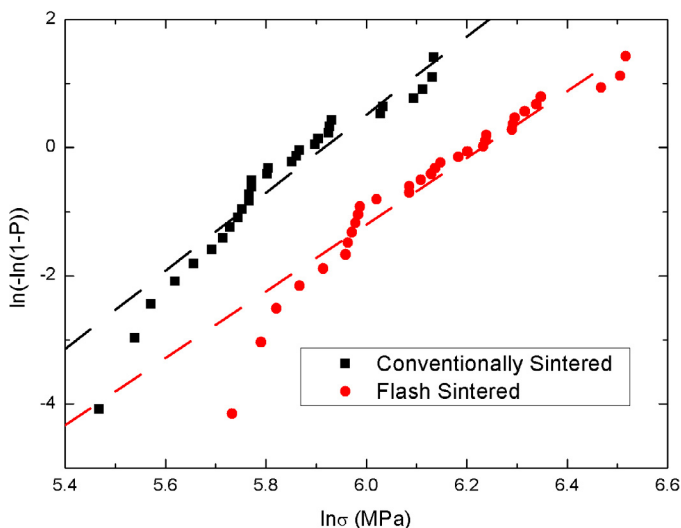

Fig. 2. Weibull diagram for flash and conventionally sintered 3YSZ.
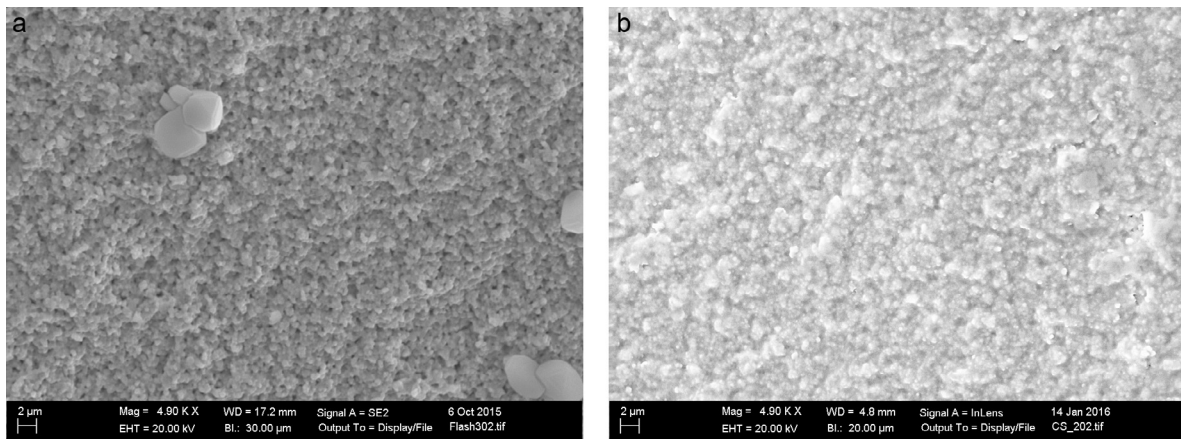
Fig. 3. SEM pictures of fracture surfaces after mechanical testing. (a) Flash sintered; (b) Conventionally sintered.

Data acquisition and parameter adjustment are possible through a system which consists of two channels for load adjustments and position regulation. Each channel could be activated separately and necessary parameter adjustments have to be done prior to a bending test. This consists of defining the maximum upper limit of the force in [N] and maximum flexure of the sample in [μm]. These parameters must be at least equal or rather higher than maximum fracture load and maximum flexure of all the samples, in order to guarantee that the maximum value lies within the defined parameter range. This could be roughly estimated by testing a few samples to the point of fracture and setting the force limit slightly higher than the fracture force measured for these samples.

Instrumental control and data acquisition are facilitated through a Labview program, which displays data received from the data acquisition system in the form of a load-flexure diagram and regulates the speed of the stepper motor. More importantly, it provides a manual function, which enables the operator to put dots on the load-flexure curve manually. These dots are placed along the curve and at the same time are recorded in the form of a text data, which provides vital information about the fracture force. The fracture force is then converted to bending strength, and fracture toughness for the notched specimens.

3. Weibull analysis and defect distribution

The analysis of the mechanical testing data of 32 samples was done via Weibull statistics. The samples were ranked due to their rupture strength and given a failure probability proportional to their rank. Those values were used to determine the Weibull parameters (modulus m and characteristic strength σ_0) using the maximum likelihood method, according to DIN EN 843 [14].

Fig. 2 is a Weibull diagram of the mechanical tests. The obtained values for Weibull modulus and characteristic strength (63.2% cumulative failure probability) are 6.09 and 371 MPa for the conventionally sintered samples, respectively, and 5.92 and 506 MPa for the flash sintered samples.

The higher characteristic strength in the case of flash sintered specimens could be explained by the different thermal history of the samples, since SEM pictures of fracture surfaces (Fig. 3) show that the grain size of the samples is alike, being $0.71 \pm 0.21\,\mu m$ for the flash sintered samples and $0.58 \pm 0.19\,\mu m$ for the conventionally sintered ones. The higher strength on flash sintered specimens could be attributed to the manufacturing method with some kind of 'tempering', since after each experiment, the samples were removed from the furnace at 900 °C to room temperature. Fig. 4 shows a cross section of a flash sintered specimen, showing two different regions, with a inner core with anomalous grains.
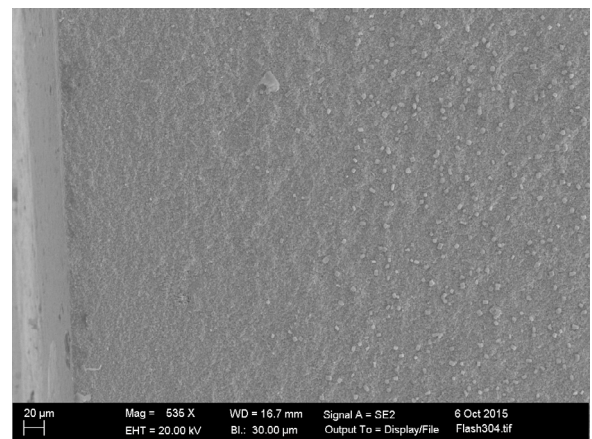

Fig. 4. Fracture surface of a flash sintered specimen, showing the two regions.

However, the grain size and porosity itself does not change on both regions. Also, the microstructural features are constant in the entire gauge length region tested.[1]

The critical defect size distribution on those samples can be calculated if the fracture toughness is known [15]:

$$K_{IC} = Y\sigma\sqrt{a} \tag{1}$$

where K_{IC} is the fracture toughness, Y is a geometrical factor σ is the failure stress and a is the critical defect size. The geometrical factor for three point notched bending was defined by Fett and Munz [16].

The notched three point bending tests yielded the values of 4.44 ± 0.32 and 4.08 ± 0.25 MPa$\sqrt{m}$ for flash and conventionally sintered specimens, respectively. Applying Eq. (1) to the Weibull test results, the defect distribution can be calculated (Fig. 5).

Both set of samples show a critical defect size lower than 80 μm, with most of the defects located on the region around 60–20 μm. there is a shift on defect size of around 20 μm from the conventionally sintered specimens to the flash sintered ones.

Since the Weibull modulus of both sets of samples is not much different, the shape of the defect distributions is alike, showing probably the same failure mechanism. The shift on the distributions cannot be explained by the difference in grain sizes, since the SEM pictures (Fig. 5) show that the grain sizes are in the same order of magnitude. That evidence points in the direction that the densification mechanism is quite similar in flash and conventional

---

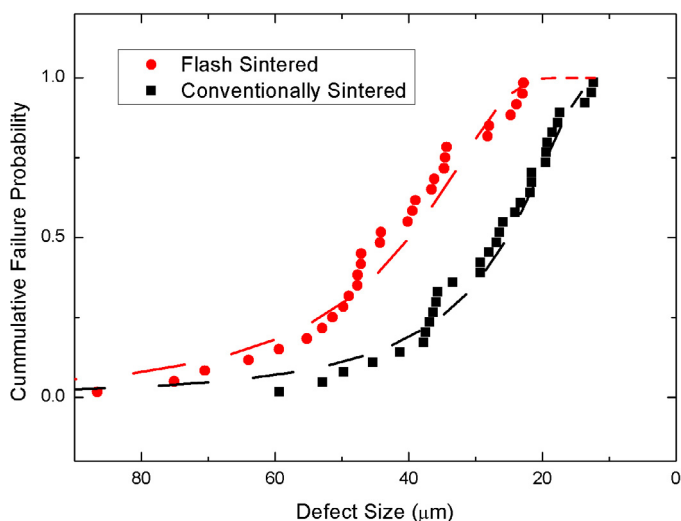[1] Addressed comment nr. 3.

Fig. 5. Calculated defect size from the Weibull distribution.

sintering, since the different process does not change the shape of the defect distribution on the material. However, care must be taken before jumping to conclusions, since the mechanical testing method does only evaluate the maximum strength and therefore the defect distribution near to the surface of the sample, which has a different thermal history from the core.

One possible explanation for the higher strength in the case of the flash sintered samples is in the sample manufacture method. Since a large number of samples was needed for this analysis, each sample was flash sintered quickly, being left in the furnace sufficient time to be in equilibrium with the furnace and then isothermally flash sintered. After sintering the sample was swiftly removed from the furnace and cooled at room temperature. This process has not caused cracks on the surface of the sample, but it could have induced residual thermal stresses which in turn can increase the effective mean strength of the material, without changing the actual defect distribution.

The difference of the average values of strength is 135 MPa. A rough estimative of the thermal stresses could be done by using the following equation:

$$\sigma_{th} = E\alpha\Delta\theta \tag{2}$$

where σ_{th} is the thermal stress, E is the elastic modulus, α is the thermal expansion coefficient and $\Delta\theta$ is the temperature gradient between the core and the surface of the sample.

Assuming $E = 200$ GPa [17] and α between 7 and $12 \cdot 10^{-6}$/K [18], leads to an average temperature gradient of 96.4 and 56.2 K, respectively, which is a reasonable figure considering the heating profiles observed.[2]

4. Effect of pore formers on flash sintering

The diagrams in Fig. 6 summarize the results of the isothermal experiments. It shows that the incubation time depends on voltage and oven temperature. The incubation time is decreasing non-linearly with increasing voltage. The higher the furnace temperature, the lower the incubation time.

In summary the diagrams in Fig. 6 do not indicate a relation between the content of pore formers and sintering behaviour on isothermal flash sintering, due to the fact that each three sets of
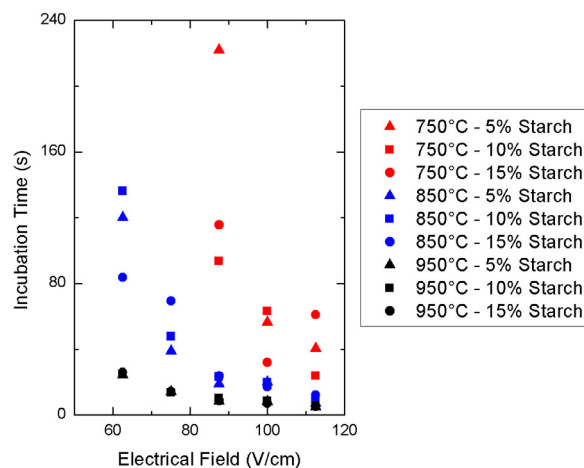
specimens differ only slightly on the incubation time for isothermal flash sintering.

The results of the constant heating rate experiments are shown in Fig. 7. It could be seen that all three sets of specimens show a similar behaviour on the onset temperature for flash sintering under constant heating rate. That indicates none or very little relation between green sample porosity and flash sintering behaviour. It is nearly the same main result as found in the isothermal flash sintering experiments.

The results have interesting implications. The fact that large pores do not influence greatly on the 'signature' phenomena in flash sintering (incubation time and onset temperature), shows that flash sintering is a quite forgiving process when dealing with preexisting defects on the green body. It can be also assumed that local field effects caused by the pores, such as local ionization and localized dielectric breakdown are not the main effects related to the onset of flash sintering, even though other researchers have shown that the atmosphere has a great role on the onset temperature for flash sintering [19].

Fig. 8 shows the pore size distribution measured from SEM micrographs on flash and conventionally sintered specimens with pore forming agents.
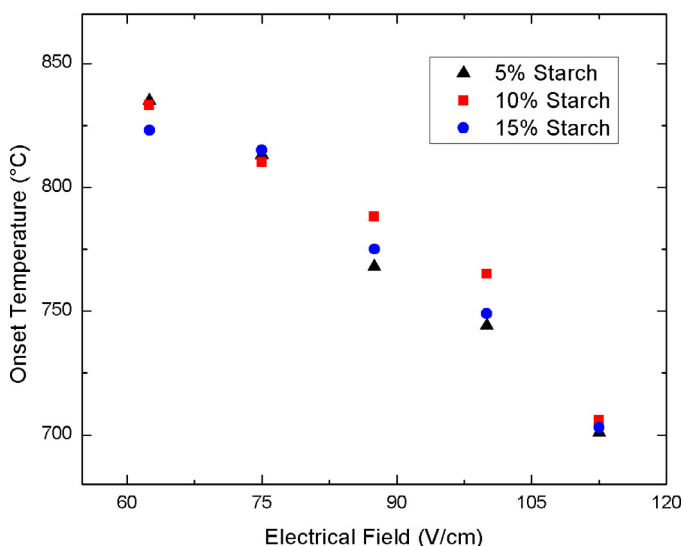

Fig. 6. Dependence of the incubation time as a function of furnace temperature and starch content.

Fig. 7. Dependence of the onset temperature for flash sintering as a function of starch content.
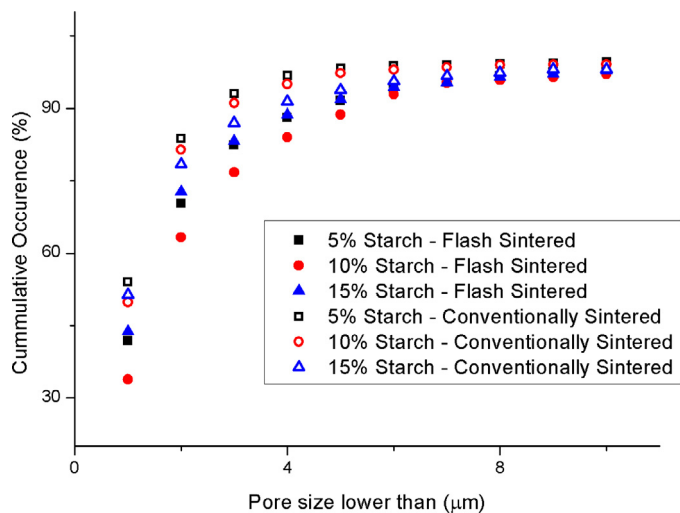
Fig. 8. Pore size distribution for flash and conventionally sintered specimens with different starch contents.

The results show that the pore size distribution of the flash sintered specimen is very close to the conventional sintered specimen, besides the much smaller pores with a diameter under 1 μm.

The second observation is that the distribution of pores with a diameter of more than 5 μm is nearly the same for all specimen of this experiment. There is no significant difference between the sintered specimen and the green samples. Since the particle size of the starch, used to increase the porosity of the specimen is up to 125 μm, these higher pore sizes are most probably caused by the starch particles. That indicates that the porosity made by the starch content remains constant through the whole sintering process for both conventional and flash sintering.

This could be explained by the recent findings that a critical conductivity should be reached for flash sintering, specially in composites [20,21]. Therefore, since the conducting path for the onset of flash sintering is mostly a bulk effect, a defect amount lower than the percolation threshold should not have a pronounced effect on flash sintering and the pore structure post sintering.

5. Summary

Related to the generation of defects during flash sintering, the mechanical testing shows that the defect distribution inferred from the Weibull modulus of flash and conventionally sintered specimens are alike, leading to a similar sintering behaviour, even though the time scales are vastly different.

The addition of pore forming agents as preexisting defects in 3YSZ green bodies does not significantly alters the main features of flash sintering, as the incubation time on isothermal experiments and the onset temperature in constant heating rate experiments. Evidence shows that those defects do not alter significantly the

green body conductivity, and therefore the critical conditions for flash sintering are achieved in similar conditions in the experimented range.

References

[1] M. Cologna, A.L.G. Prette, R. Raj, Flash-sintering of cubic yttria-stabilized zirconia at 750 °C for possible use in SOFC manufacturing, J. Am. Ceram. Soc. 94 (2011) 316–319.

[2] M. Cologna, B. Rashkova, R. Raj, Flash sintering of nanograin zirconia in <5 s at 850 °C, J. Am. Ceram. Soc. 93 (2010) 3556–3559.

[3] M. Cologna, J.S.C. Francis, R. Raj, Field assisted and flash sintering of alumina and its relationship to conductivity and MgO-doping, J. Eur. Ceram. Soc. 31 (2011) 2827–2837.

[4] A.L.G. Prette, M. Cologna, V. Sglavo, R. Raj, Flash-sintering of Co$_2$MnO$_4$ spinel for solid oxide fuel cell applications, J. Power Sources 196 (2011) 2061–2065.

[5] R.I. Todd, E. Zapata-Solvas, R.S. Bonilla, T. Sneddon, P.R. Wilshaw, Electrical characteristics of flash sintering: thermal runaway of joule heating, J. Eur. Ceram. Soc. 35 (2015) 1865–1877.

[6] J. Narayan, A new mechanism for field-assisted processing and flash sintering of materials, J. Scr. Mater. 69 (2013) 107–111.

[7] S.K. Jha, The effect of electric field on sintering and electrical conductivity of titania, J. Am. Ceram. Soc. 97 (2) (2014) 527–534.

[8] H. Yoshida, Y. Sakka, T. Yamamoto, J.M. Lebrun, R. Raj, Densification behaviour and microstructural development in undoped yttria prepared by flash-sintering, J. Eur. Ceram. Soc. 34 (2014) 991–1000.

[9] K.S. Naik, V.M. Sglavo, R. Raj, Flash sintering as a nucleation phenomenon and a model thereof, J. Eur. Ceram. Soc. 34 (15) (2014) 4063–4067.

[10] K. Terauds, J.-M. Lebrun, H.-H. Lee, T.-Y. Jeon, S.-H. Lee, J.H. Je, R. Raj, Electroluminescence and the measurement of temperature during Stage III of flash sintering experiments, J. Eur. Ceram. Soc. 35 (11) (2015) 3195–3199.

[11] J.S.C. Francis, M. Cologna, R. Raj, Particle size effects in flash sintering, J. Eur. Ceram. Soc. 32 (12) (2012) 3129–3136, ISSN 0955-2219.

[12] J.S.C. Francis, A study on the phenomena of flash-sintering with tetragonal zirconia (PhD Thesis), University of Colorado at Boulder, 2013.

[13] H. Jelitto, F. Felten, M.V. Swain, H. Balke, G.A. Schneider, Measurement of the total energy release rate for cracks in PZT under combined mechanical and electrical loading, J. Appl. Mech. 74 (2007) 1197–1211.

[14] DIN EN 843 Standard, Advanced Technical Ceramics – Mechanical Properties of Monolithic Ceramics at Room Temperature, 2007.

[15] D. Munz, T. Fett, Ceramics. Corr. 2. Print, Springer, Berlin, 2001.

[16] T. Fett, D. Munz, Stress Intensity Factors and Weight Functions, Computational Mechanics Publications, Southampton, 1997, pp. 108ff.

[17] J.W. Adams, R. Ruh, K.S. Mazdiyasni, Youngs modulus, flexural strength, and fracture of yttria stabilized zirconia versus temperature, J. Am. Ceram. Soc. 80 (4) (1997) 903–908.

[18] H. Hayashi, T. Saitou, N. Maruyama, H. Inaba, K. Kawamura, M. Mori, Thermal expansion coefficient of yttria stabilized zirconia for various yttria contents, Solid State Ionics 176 (56) (2005) 613–619.

[19] Y. Zhang, J. Luo, Promoting the flash sintering of ZnO in reduced atmospheres to achieve nearly full densities at furnace temperatures of 120 °C, Scr. Mater. 106 (2015) 26–29.

[20] S.K. Jha, R. Raj, Electric fields obviate constrained sintering, J. Am. Ceram. Soc. 97 (2014) 3103–3109.

[21] E. Bichaud, J.M. Chaix, C. Carry, M. Kleitz, M.C. Steil, Flash sintering incubation in Al$_2$O$_3$/TZP composites, J. Eur. Ceram. Soc. 35 (9) (2015) 2587–2592.